

Inelastic Incoherent Neutron Scattering Studies of Water Interacting with Biological Macromolecules

Stuart V. Ruffle,^{†,‡} Ilias Michalarias,[§] Ji-Chen Li,[§] and Robert C. Ford^{*,†}

Contribution from the Department of Biomolecular Sciences and the Department of Physics, UMIST, P.O. Box 88, Manchester M60 1QD, U.K.

Received May 25, 2001. Revised Manuscript Received November 16, 2001

Abstract: The interaction between water and biological macromolecules in living organisms is of fundamental importance in a range of processes. We have studied water–DNA and water–proteolipid membrane systems over a range of hydration states using inelastic incoherent neutron scattering. We find a relatively sharp transition for both systems at a water concentration above which bulk solvent can be detected. Below this concentration, bulk water is essentially absent, i.e., all the water in the system is interacting with the biological macromolecules. This water is strongly perturbed as judged by its energy transfer spectrum, with a broader and lower energy transition than bulk water in the 50–75 meV (~ 400 – 600 cm^{-1}) range. Taking into account the differing geometry of (cylindrical) DNA and (planar) membranes, the number of water shells perturbed by each system was estimated. A conclusion is that in living organisms a large proportion of the cellular water will be in a state quite distinct from bulk water. The data add to the growing evidence that water structure in the vicinity of biological macromolecules is unusual and that the proximal water behaves differently compared to the bulk solvent.

Introduction

Cells in living organisms are environments that are composed of very high concentrations of macromolecules such as RNA, DNA, and protein as well as membranes.^{1,2} Estimates for, e.g., protein concentrations in the cytoplasm of the cell are about 200–300 mg of protein/mL, leading to a gellike consistency. The problems and advantages of maintaining such molecular crowding within the cellular milieu have been discussed in depth.^{1,2} Where high water content is functionally required in cells (e.g. in generating turgor pressure in plant cells), the bulk water tends to be segregated into separate compartments in the cell (vacuoles in this case). This suggests that a high macromolecule/low water situation may be important for cellular function. The concept that molecular crowding could facilitate many cellular processes has been explored previously.^{1,2} Water structure has been extensively studied in its pure form by neutrons,^{3–5} but studies of water–water and water–macromolecule interactions under conditions similar to those found in the cell are rarer, despite being of considerable significance.

There is a growing body of evidence that the structure and behavior of water in the vicinity of biological macromolecules may be different from that of pure water. High-resolution crystal

structures of pure protein or DNA that have been obtained at cryogenic temperatures have ordered interfacial water molecules in the electron density maps, and in a few cases these represent a large fraction of the total solvent content^{6,7} in the crystals. However, these ordered water molecules do not form the typical ice Ih structure, but rather are involved in many different forms of hydrogen bonding networks with the macromolecule and with each other.^{6–8} If such an altered water structure exists in the vicinity of macromolecules in cells, then it has potential significance for a range of fundamental functions such as protein folding and stability, DNA packaging, and molecular recognition. Moreover, an understanding of the interaction of water and macromolecules at cryogenic temperatures is, in its own right, of considerable importance, especially for the freezing of cells and tissues without the irretrievable loss of function.

Experimental investigation of water around DNA and proteins is traditionally difficult. Using diffraction (X-ray or neutron) techniques is very difficult for this type of study, because first, although (synchrotron) X-ray diffraction has a better resolution and luminosity, lack of ability to see protons makes it very unsuitable for examining the structure of water (the orientations of water molecules in particular). Neutron scattering, on the other hand, has the ability to see proton positions; however, the complex structures of DNA/proteins and the arrangements of water molecules around them make it very hard to gain a clear picture of the spatial arrangements as often averaged (time

* Corresponding author. E-mail: r.ford@umist.ac.uk.

[†] Department of Biomolecular Sciences, UMIST.

[‡] Present address: School of Biological Sciences, University of Exeter, Exeter EX4 4PS, U.K.

[§] Department of Physics, UMIST.

(1) Ellis, J. R. *Curr. Opin. Struct. Biol.* **2001**, *11*, 114–119.

(2) Burg, M. C. *Cell Physiol. Biochem.* **2000**, *10*, 251–256.

(3) Li, J. C.; Ross, D. K. *Nature* **1993**, *365*, 327–329.

(4) Li, J. C. *J. Chem. Phys.* **1996**, *105*, 6637–6657.

(5) Kolesnikov, A. I.; Li, J. C.; Parker, S. F.; Eccleston, R. S.; Loong, C. K. *Phys. Rev. B* **1999**, *59*, 3569–3578.

(6) Esposito, L.; Vitagliano, L.; Sica, F.; Sorrentino, G.; Zagari, A.; Mazzarella, L. *J. Mol. Biol.* **2000**, *297*, 713–792.

(7) Clark, G. R.; Squire, C. J.; Baker, L. J.; Martin, R. F.; White, J. *Nucleic Acids Res.* **2000**, *28*, 1259–1265.

(8) Soler-Lopez, M.; Malinia, L.; Subirana, J. A. *J. Biol. Chem.* **2000**, *275*, 23034–23044.

and molecule) positions are given. However, using neutron vibrational spectroscopy, we can define the local structures of water molecules by comparing the vibrational signatures with known configurations in high-pressure phases of ice.^{3–5} The neutron spectrum (predominated by H motion) in the low-frequency region is mainly due to H-bonding between water and DNA/proteins, or between water and water molecules. Inelastic incoherent neutron scattering (IINS) can be employed as a vibrational spectroscopy method that provides information in the same energy ranges as infrared and Raman spectroscopies.^{9,10} The advantage of using neutron spectroscopy is that its intensity is directly proportional to the phonon density of states which can be rigorously calculated by using lattice or molecular dynamical methods based on a known potential function (i.e. no selection rules are needed as in the IR and Raman methods).¹¹

A drawback to IINS, however, is that it is difficult to generate neutron fluxes that are sufficiently high for good signal/noise spectra and hence it suffered poor resolution. However, the increased proton flux on ISIS and sensitive detection facilities provided by the newly developed TOSCA spectrometer at the Rutherford Appleton Laboratory have recently overcome this barrier, provided that large (gram) quantities of sample can be produced. Studies of biological samples, which are rich in hydrogen, are thus possible. By comparing with spectra measured for the protein or DNA samples at different dehydration levels with different exotic structures of ice, we can understand the local structural characteristics of water around the biomolecules.

Experimental Methods

The studies herein described have been performed for both the nonhydrated and hydrated state of two systems, a biological membrane and DNA. Biological membranes are extremely diverse in terms of morphology and composition. We have initially chosen “grana” membranes isolated from higher plant leaves as our material for the studies of water–membrane interactions.¹² These membranes were chosen for the following reasons: (a) The membranes can be purified in large (gram) quantities. They are readily pelleted by centrifugation and therefore exchange of solvent is possible as well as the preparation of very concentrated material.¹² (b) They are relatively homogeneous, being composed of one major protein complex, with a high protein:lipid ratio. (c) Their architecture is well characterized by electron microscopy and by low-angle X-ray and neutron scattering studies.¹² They are isolated as paired planar sheets that are open on both sides of the membrane to water (i.e. they are unsealed). Each membrane sheet is approximately 8 nm across and extends on average 300 × 300 nm in the plane. This morphology therefore avoids complications due to secluded water volumes that would arise with vesicular membrane preparations.

The membranes were prepared from market spinach following the method of Berthold et al.¹⁷ with the modifications of Ford and Evans.¹⁸

Leaves were washed in cold water and destemmed, and the larger leaves were stripped of their major leaf ribs. The leaves were ground for 15 s in a Waring blender in ice cold grinding buffer, 0.33 M sorbitol, 0.2 mM MgCl₂, 20 mM 2-(*N*-morpholino)ethanesulfonic acid (MES)–NaOH; pH 6.5 with 5 mM ascorbate. The blended material was filtered through eight layers of muslin and then centrifuged at 3000 × g for 5 min at 4 °C. All buffers were cold (≈4 °C) when used and all stages of the preparation, after the harvesting of the chloroplasts, were kept in as near dark conditions as possible to minimize oxidative damage to the membranes and protein complexes.

The pelleted chloroplasts were resuspended in 5 mM MgCl₂ hypotonic solution for 1 min to osmotically shock the organelles and release the thylakoid membranes. This mixture was then diluted 1:1 with double strength grinding buffer. The thylakoids were harvested as a pellet by centrifugation at 3000 × g for 20 min at 4 °C. The pellet was thoroughly resuspended in 25 mM NaCl, 5 mM MgCl₂, 20 mM MES–NaOH; pH 6.3 (RM) and incubated on ice, in the dark for 90–120 min to allow the lateral segregation of the thylakoid membrane protein complexes.

The stacked membranes were incubated at 4 °C for 25 min after the addition of resuspending medium and Triton X-100 (20% (w/v) stock in distilled water) to final concentrations of 2 mg/mL of chlorophyll and 25:1 Triton to chlorophyll (w/w). The mixture was centrifuged at 4 °C for 30 min at 40 000 × g to harvest the photosystem II–enriched grana membrane fragments. The grana membranes were resuspended into RM and the centrifugation repeated. After lyophilization for 12 h, membranes were loaded into aluminum sample holders. Dehydrated samples were prepared by loading lyophilized Deoxyribonucleic acid Sodium Salt produced from Salmon testes (formerly known as type III and purchased from SIGMA) or lyophilized membranes into aluminum sample cans that were fitted with an airtight valve and then connected to a vacuum system. The lyophilized samples were evacuated for 1 day at –20 °C at a pressure of ~10^{–4} bar, and the mass of the canister and the internal pressure were monitored. After closure of the valve, the samples were stored at –80 °C under vacuum.

A series of experiments with a microbalance instrument (IGA, manufactured by Hiden Analytical Ltd, Warrington, U.K.) demonstrated that after applying these conditions the samples were essentially devoid of water. Hydration of the samples was carried out by fully opening the can to atmosphere and incubating the hygroscopic material at room temperature for various time periods. For the higher hydration levels distilled water was directly added to the sample and then allowed to equilibrate for >1 h. Hydration levels were determined by measuring the mass change upon hydration.

Data were collected at <30 K at the TOSCA experimental station at ISIS¹⁹ and the collection time was between 6 and 12 h for each spectrum depending on the sample sizes and hydration level, except for one sample (35 g of water/100 g of membranes) where beam time restrictions allowed only ~2 h. After subtraction of background, all data were averaged into 1 meV bins, which does not compromise the resolution of the instrument. Since sampling is progressively finer at lower energies with the TOSCA instrument, the averaging of our data is greater at lower energies, as can be observed in Figures 1–3.

Results

The series of IINS measurements were performed on TOSCA at ISIS for both samples (Grana membranes and DNA) at different hydration levels as shown in Figure 1 in the energy transfer range from 3 to 200 meV at <30 K. The spectrum of ice Ih is also plotted on top of the figure for comparison

(9) Goupil-Lamy, A. V.; Smith, J. C.; Yunoki, J.; Parker, S. F.; Kataoka, M. *J. Am. Chem. Soc.* **1997**, *119*, 9268–9273.

(10) Middendorf, H. D.; Hayward, R. L.; Parker, S. F.; Bradshaw, J.; Miller A. *Biophys. J.* **1995**, *69*, 660–673.

(11) Li, J. C.; Tomkinson, J., In *Molecular Dynamics—from Classical to Quantum Methods*; Balbuena, P. B., Seminario, J. M., Eds.; Elsevier Scientific, plc: Amsterdam, 1999; pp 471–532.

(12) Nicholson, W. V.; Ford, R. C.; Holzenburg, A. *Biosci. Rep.* **1996**, *16*, 159–187.

(13) Marechal, Y. *J. Mol. Struct.* **1997**, *416*, 133–143.

(14) Brovchenko, I.; Paschek, D.; Geiger, A. *J. Chem. Phys.* **2000**, *113*, 5026–5036.

(15) Hayward, S.; Kitao, A.; Hirata, F.; Go, N. *J. Mol. Biol.* **1993**, *234*, 1207–1217.

(16) Cheng, Y. K.; Rossky P. J. *Nature* **1998**, *392*, 696–699.

(17) Berthold, D. A.; Babcock, G. T.; Yocum, C. F. *FEBS Lett.* **1981**, *134*, 231–234.

(18) Ford, R. C.; Evans, M. C. W. *FEBS Lett.* **1983**, *160*, 159–163.

(19) Parker, S. F.; Carlile, C. J.; Pike, T.; Tomkinson, J.; Newport, R. J.; Andreani, C.; Ricci, F. P.; Saccetti, F.; Zoppi, M. *Physica B* **1998**, *241–243*, 154–156.

Table 1. Summary of the Major Features (peaks, broad collections of peaks, and transitions) of the IINS Spectra of Ice Ih, Membranes, and DNA, Measured at <30 K on the TOSCA Spectrometer^a

energy (meV)	sample	putative vibrational mode(s)—see references	ref
7.1	I	acoustic phonon region	3, 4
10	M, D	acoustic phonon region	9, 10
28.4	I	H bond (weak)	3, 4
37.9	I	H bond (strong)	3, 4
22–40	M, D	CH ₃ torsion	9
67	I	H bond librational band left edge	3, 4
50–65	M	coupled protein skeletal and dihedral displacements	9
70	M	?	
83	M	?	
121	I	H bond librational band right edge	3, 4
90–140	M, D	CH ₃ -r, CH ₂ -r, NH-ip, NH-op, NH ₂ -b, NH ₂ -r	9, 10
145–190	M, D	CH-b, CH ₂ -b, CH ₂ -w, CH ₂ -tw, CH ₃ -sb, CH ₃ -ab, amide II and III (NH-ib coupled to C–N stretch)	9, 10

^a Key: I = ice Ih. M = membranes. D = DNA. Vibrational modes: -r, rocking; -ip, in-plane bend; -op, out-of-plane bend; -b, bend; -w, wagging; -tw, twisting; -sb, symmetric bending; -ab, asymmetric bending.

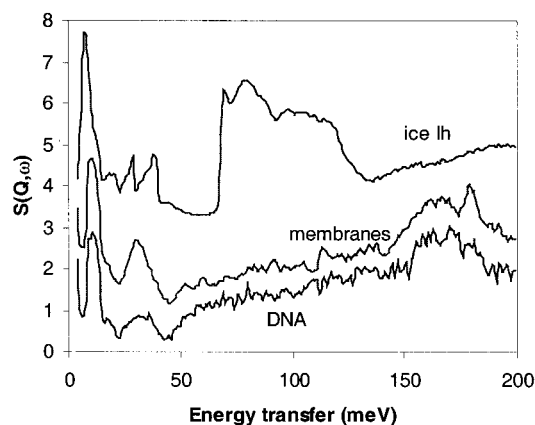


Figure 1. IINS spectra in the energy transfer range of 3–200 meV (~ 24 – 1600 cm^{-1}) for pure water, dry grana membranes, and dry DNA measured at <30 K. A description of the various peaks in the spectra is given in Table 1. Data are averaged into 1 meV bins.

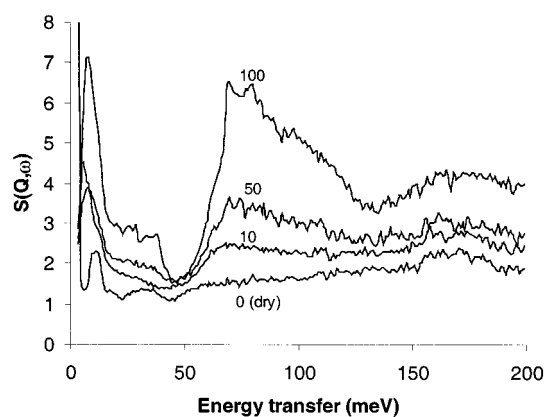


Figure 3. IINS spectra for DNA at increasing levels of hydration corresponding to 0 (dry), 10, 50, and 100 g of water per 100 g of dry DNA. All data have been averaged into 1 meV bins, and normalized as described in the text.

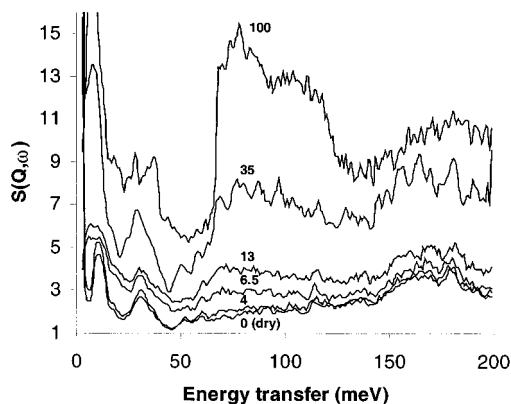


Figure 2. IINS spectra for grana membranes at increasing levels of hydration. The spectra shown are for 0 (dry), 4, 6.5, 13, 35, and 100 g of water per 100 g of dry membranes. The data are averaged in 1 meV bins except for the data at 35 g of water/100 g of membranes, which are in 3 meV bins. The latter data were collected for a relatively short time period compared to the other spectra and have a poorer signal/noise ratio. The spectra have been normalized as described in the text.

purposes. Grana membrane composition is known to be complex, with lipid, protein, and pigment (chlorophyll and carotenoid) present. This is reflected in the IINS data that show multiple peaks, as listed in Table 1. Examination of several spectra for these membranes suggests that many weaker peaks are unresolved at higher energy transfer (above 100 meV), and data for the high-energy region (100–500 meV) collected on

the HET spectrometer at the neutron spallation source at the Rutherford Appleton Laboratory have recently confirmed this. The spectrum for the membranes is quite similar to earlier spectra recorded for protein samples, with good signal/noise ratios.⁹ The simpler composition of DNA is reflected in the IINS spectrum that shows fewer and relatively broad peaks. A strong peak at ~ 10 meV is common to both the DNA and grana membrane spectrum which is associated with acoustic phonons (i.e. global vibrations). Detailed assignment of the various peaks has been attempted in Table 1, drawing on the previous study by IINS of a dry globular protein⁹ (*Staphylococcus aureus* nuclease) and rat collagen.¹⁰ The IINS spectra of pure water (in this case in its normal ice Ih form) has been previously characterized⁴ and some of the peaks are also included in Table 1. The ice spectrum has sharp and intense peaks that dominate the IINS spectrum for well-hydrated protein or DNA solutions (see e.g. Figures 2 and 3).

In spectra for both dry DNA and dry membrane samples, peaks around 170–180 meV are observed that probably correspond to a mixture of bending, twisting, and wagging motions of $-\text{CH}$, $-\text{CH}_2$, and $-\text{CH}_3$ groups⁹ as well as the amide I, II, and III bands¹⁰ (see Table 1). In pure water (ice Ih spectrum), this region shows only a broad upward trend from 130 to 190 meV, with no discrete peaks (Figure 1). There is therefore little overlap between features due to water and DNA/membrane in the region around 145–190 meV. In hydration studies, peaks in this region could be inferred as nonwater and

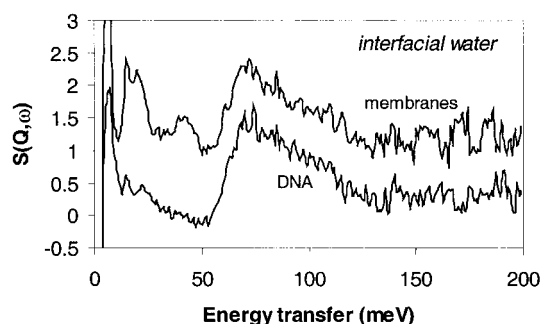


Figure 4. Estimation of the IINS spectra for interfacial water in hydrated membranes (13 g of water/100 g of membranes) and hydrated DNA (50 g of water/100 g of DNA). Spectra are obtained after subtraction of the dry membranes or DNA component (see Figure 1). Data are averaged into 1 meV bins.

therefore could be employed for the normalization of different spectra used for the deconvolution of the water component. This makes the assumptions that the DNA (or membrane) component in this energy transfer region will be relatively unaffected by the presence of water, and vice versa for the water component. These assumptions seem crude, but reasonably well justified as illustrated by the data in Figure 2 where a hydration series is shown for grana membranes. The two peaks at 170 and 180 meV in the spectrum remain very similar in terms of relative strength and position over a broad range of water concentrations. Similar results were also obtained for DNA (Figure 3). FTIR studies of protein in this energy range¹³ and previous IINS studies of collagen¹⁰ also suggest that these peaks due to C–H motions are relatively unaffected by hydration.

Spectra for the two biological systems under study recorded at different levels of hydration are presented in Figures 2 and 3. The sharp peaks of the ice Ih spectrum, corresponding to bulk water, are clearly observed in the higher hydration states for both types of sample (cf. Figure 1). However, at lower hydration levels, the sharp ice Ih peaks appear to be completely absent, rather than proportionately reduced. After subtraction of the dry DNA or dry membrane signal, it is clear that at the lower hydration levels, the water spectrum is drastically altered compared to the bulk water (ice Ih) signal (see Figure 4). The main feature of the difference spectrum for water/DNA is a

broad increase from ~54 meV up to a peak at 73 meV. There is little or no evidence for the sharp transitions at 28, 37, and 65 meV that characterize this region of the bulk water spectrum. For the water/membrane difference spectrum, a very similar feature with a peak at ~71 meV is observed, with no indication of the sharp transition at 65 meV. However, other features can be discerned in the difference spectrum, notably peaks at around 28 and 37 meV. The bulk water signal in this region is dominated by two peaks associated with stretching of strong and weak hydrogen bonding (O–H···O).^{3,4} If the two peaks in the interfacial water signal in grana membranes correspond to similar hydrogen bonding interactions, then they are also significantly broadened. However, the absence of these peaks in the interfacial water signal in DNA samples indicates that hydrogen bonds in these water structures are perturbed considerably from the bulk state. Clearly, further studies are required to better characterize these interactions.

Plots of the water concentration dependence of the magnitude of the broad 50–73 meV transition associated with interfacial water and the sharp 65 meV transition associated with bulk water are presented in Figure 5. In both hydration experiments, bulk water signals are not detected below a certain water concentration. At lower concentrations, the vibrational spectra indicate that all of the water molecules are perturbed. At concentrations of water above this point, bulk water can be detected, although the spectra indicate that interfacial water continues to accumulate toward a saturation level. For the grana membranes, the transition point where bulk water is detected occurs at ~13 g of water/100 g of dry membranes, while for the DNA sample, it occurs at a significantly higher level (~50 g of water/100 g of dry DNA).

Discussion

Estimates of the number of water shells surrounding the DNA and the membranes suggest that 1 to 4 layers of water molecules comprise the interfacial water signal detected. The observation that the transition from interfacial to bulk water occurs at a higher water concentration in the DNA samples may be crudely understood in terms of the different structures of the two. While DNA has a long cylindrical shape of diameter ~2 nm, the grana

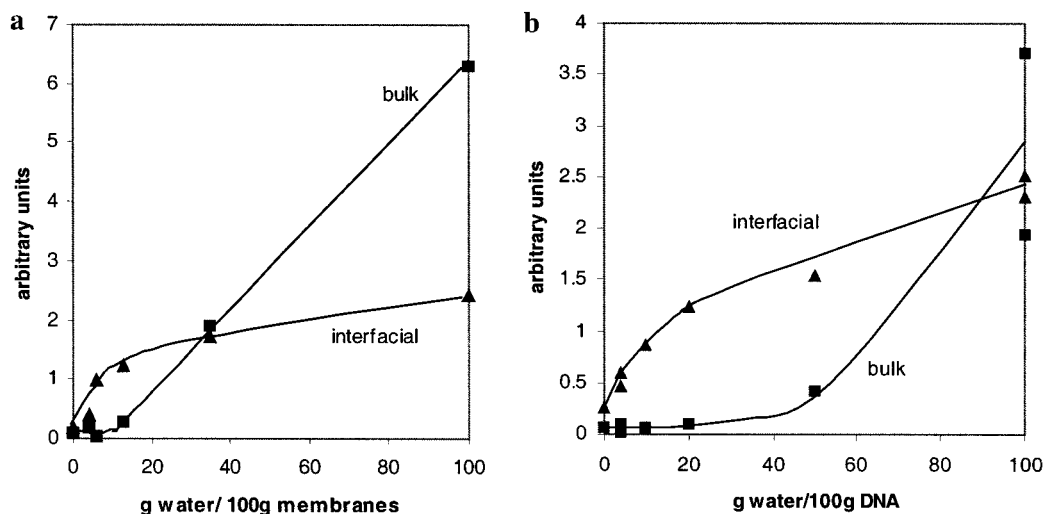


Figure 5. Bulk water and interfacial water signal magnitudes as a function of hydration of (a) grana membranes and (b) DNA. Bulk water (boxes) is measured by the sharp rise at 66–69 meV, while interfacial water (triangles) is given by the magnitude of the broad increase from 50 to 73 meV (from which any bulk signal is subtracted).

membranes consist of extensive planar sheets of thickness ~ 8 nm. To a first approximation, the surface area/mass ratio of DNA will be much higher than that of the membrane system. For example, a single layer of interfacial water molecules 0.25 nm thick would add $\sim 56\%$ to the volume of the dry DNA cylinder but only 6% to the volume of the membranes. Thus the transitional points in Figure 5 correspond to about 2 water layers (on each side) for grana membranes and about 1 layer for the DNA. For both systems the interfacial water signal saturates at approximately double the transitional level, implying with these rough estimates that up to ~ 4 water layers for the membranes and up to ~ 2 layers for the DNA may be perturbed from the bulk state. These estimates of the number of water layers do not take into account the differences in the charge and surface topology of the DNA compared to membranes, and thus these preliminary calculations based on geometry must be treated with caution. However, our preliminary studies for a globular protein have so far confirmed that estimation of interfacial water based on geometrical considerations is a reasonable starting point.

Extrapolating these estimates of interfacial water back to the cell, it becomes clear that a large proportion of the cytoplasmic water will behave differently than bulk water. In the nucleus of eukaryotes where DNA and protein levels are very high, then it can be predicted that the majority of the water molecules will be perturbed. In mitochondria, cellular compartments involved in energy metabolism, the overall protein concentration is estimated to be ~ 560 mg/mL, a level equivalent with that found in protein crystals,^{1,2} suggesting that almost all water molecules would be perturbed in mitochondria.

The structure of the interfacial water that gives rise to the broadened IINS spectra (Figure 4) is unclear at present. A detailed theoretical analysis is now possible, but beyond the scope of this paper. Low-temperature crystallographic studies of water bound in crystals of protein and DNA have revealed structures that are consistently different from that of ice Ih.^{6–8}

It should be possible to calculate the IINS spectra for these ordered water molecules and to compare the experimental (Figure 4) and calculated spectra. However, disordered water molecules are also present in the crystals, and it is feasible that they also contribute to the interfacial water signal. Molecular dynamics simulations might offer an alternative route to explore potential structures for these disordered water molecules.^{14,15}

Ordered water molecules in oligonucleotide (short DNA) crystals take up hydrogen-bonded polygonal structures, with pentagonal organization predominating.^{7,8} In the most dehydrated DNA crystals, solvent content is as low as $\sim 20\%$,⁷ which suggests that all the water molecules are nonbulk (cf. Figure 5). Protein crystals rarely diffract X-rays to resolutions that allow hydrogen atoms to be assigned. However, a few ultrahigh resolution structures are available, and these have revealed the water molecules surrounding and interacting with the protein in the crystals. Five- and six-membered rings of water molecules are detected, particularly near hydrophobic groups. Occasional large hydrogen-bonded networks with a clathrate cage structure are also observed.^{6–8,16} Most ordered water molecules are observed in the first shell, i.e., within 0.3 nm of the nearest protein atom. However, a significant percentage of ordered water molecules can be observed in higher shells, with no direct protein contacts.⁶ It is therefore not unreasonable to suspect that the perturbation of bulk water by protein or DNA can extend to more than one shell of water molecules.

Acknowledgment. We thank Drs. Stewart Parker and Daniel Colognesi for their help and expert assistance at the TOSCA experimental station within the ISIS pulsed neutron facility (Rutherford Appleton Laboratory, Oxford, U.K.). The work was supported by the U.K. Biotechnology and Biological Research Council.

JA016277W